Indian Journal of Engineering & Materials Sciences
Vol. 29, December 2022, pp. 826-831
DOI: 10.56042/ijems.v29i6.70278

Hot Deformation Behavior and Strain Rate Sensitivity of α+β Brass Sheet by Uniaxial Material Constitutive Equations

Bandhavi Challa*, & Srinivasa Rao Seeram

Department of Mechanical Engineering, Koneru Lakshmaiah Education Foundation, Guntur 522 302, India

Received: 9 September 2022; Accepted: 17 October 2022

The present work proposes a systematic procedure for evaluation of high temperatures deformation and formability of α+β Brass undergoing the uniaxial tensile test conditions. Firstly, uniaxial tensile tests were conducted on Universal Testing Machine (UTM) with loading capacity of 100 KN at temperature of 773K, 873K and 973K with a quasi-static strain rates of $0.001s^{-1}$, $0.01\ s^{-1}$ and $0.1s^{-1}$. Hot tensile flow stress behaviors have been affected significantly by test temperatures and strain rates for Brass. Drop-in yield and ultimate tensile strength have been observed at approximately 58 % and 68 % with a rise in test temperature from 773 K to 973 K. Around 30% improvement has been observed in % elongation with rise in test temperature. Further, flow stress has been predicted by most popular Johnson Cook (JC) uniaxial constitutive model at wide range of temperatures (773K, 873K and 973K) and strain rates ($0.001s^{-1}$,$0.01\ s^{-1}$ and $0.1s^{-1}$). Further, yield loci have been plotted at various temperatures using Hill 1948 and Barlat 1989 yield function. Barlat 1989 has followed experimental results correctly in all test temperatures.

Keywords: Johnson-Cook model, Tensile test, Yield function

1 Introduction

In recent times, a complex and creative product normality has been affected the manufacturing industries and sheet metal forming industries with increase in the demand and people's interest. Most favourite geometrical products parts such as automobile bodies and kitchen utensils are totally perplexing and diversified recently. Not only non-simple shape but also reduced weight is primary focus for green society and less energy consumption. Developed alloy such as brass alloy, a substitutional alloy for copper, are more popular due to comparatively light weight and with exceptional variation in mechanical and electrical properties[1-3]. Brass exceptionally used for the marine applications namely, sea valve stem, rigs ammunition components, wear strips and boats. This alloy is used to manufacture the musical instruments, horns, doorknobs, fashion jewellery, architectural panels, switches, and bells[4-6]. Self-corrosion or blackish tarnish, a non-destructive phenomenon where oxidation of brass occurs, is the main failure mechanism noticed for the brass. However, the biggest challenge is the removal of tarnish to upkeep brass.

*Correspondence author
(E-mail: challa.bandhavi@gmail.com)

Brass exhibits a typical plasticity due to complex microstructure[5, 7-9]. For cost effective manufacturing of brass alloy part, researcher emphasized on deformation behaviour and failure aspect of the alloy under wide range of temperature and strain rates[5,8,10]. Most of the reported literature described the loss of ductility with increase in tensile strength for strain hardening of alloy[11,12]. To improve the ductility of material, one of the prominent solutions is testing at elevated temperatures. Elevated temperature makes alloy softer which easier to mould to desired shape and size[13,14]. Also, selection of optimal process parameters for effective production of complex shape is very necessary. Some of the literature reported the effect of dynamic and intermediate strain rates on the deformation behaviour of alloy[15,16]. However, mechanical properties under quasi-static rates still unstudied in detail for the industrial forming applications.

Padmavardhani and Prasad[17] reported the influence of strain rate and temperature on tensile flow behavior of α +β brass and β brass. Drop in the tensile strength has been observed with decrease in strain rates (10^{-3} –$10^{2}\ s^{-1}$) and increase in temperatures 550ºC-800 ºC. Further, effect of strength and total elongation on annealed hetero-structured brass at strain rates $5 \times 10^{-4}\ s^{-1}$ has been considered Fang et al.[18] Xiao et al.[16] investigated the hot deformation

behaviour of H62 brass alloy by uniaxial Arrhenius-type constitutive equations for temperature 650–800 ºC. Furthermore, significance of Zinc percentage in Brass alloy on ductility and material strength has been investigated by the Rehren et al.[5]. Also, malleability of α+β Brass alloy mainly depends upon the zinc percentage.

After a through literature review, it is noticed that that the no considerable reports have been reported on influence of the process parameters on hot deformation and formability evaluation of α+β Brass alloy. Thus, present work is mainly focused on the systematic procedure for evaluation of high temperatures deformation of α+β Brass undergoing the stretch forming process. Firstly, flow stress have been predicted by most popular Johnson Cook (JC) uniaxial constitutive model at wide range of temperatures (773K, 873K and 973K) and strain rates (0.001 s^{-1},0.01 s^{-1} and 0.1 s^{-1}).

2 Materials and Methods

Commercially available cold rolled α+β Brass alloy sheet of 1 mm thickness, with alloying elements Cu (61.64%), Zn (38.14%), Fe (0.075%), Pb (0.068%), and some other impurities, were considered in present study. The test sample for microstructural analysis were prepared as per the ASTM E3-95 standards. Fig. 1 shows basic microstructure of parent Brass alloy sheet.

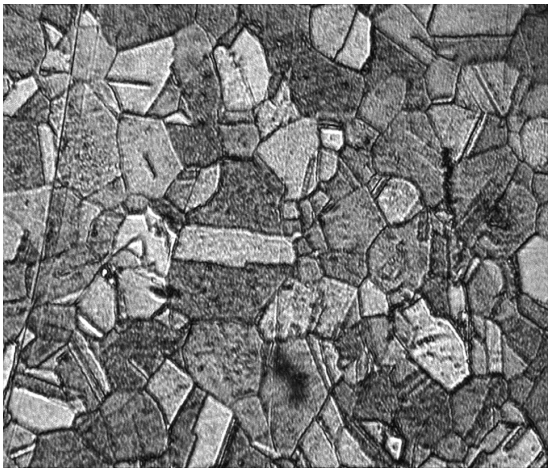

Fig. 1 — Optical microstructure of parent Brass alloy.

Uniaxial tensile samples are wire cut using EDM machine as per ASTM E08/E8 M-11 standards with a dimension as per Fig. 2(a). All dimensions are mentioned in mm. In order to consider the material anisotropy, specimens were wire cut along three different directions such as rolling (0º), transverse (45º) and normal (90º) directions with respect to the rolling direction as shown in Fig. 2(b). Uniaxial tensile tests were conducted on Universal testing machine (UTM) with loading capacity of 100 KN at temperature of 773K, 873K and 973K with a quasi-static strain rates of 0.001s^{-1}, 0.01 s^{-1} and 0.1s^{-1}. The UTM was equipped with two zone split furnace, maximum 1000 °C heating capacity with ± 3 °C accuracy.

Effect of strain rate and test temperature on flow stress behavior was analyzed. Figure 3 displays effect of test temperatures (773 K, 873 K, and 973 K) on tensile flow behavior of Brass for various strain rates. It was noticed that rise in test temperature significantly affect speak flow/yield stress. Yield

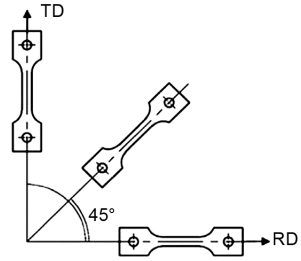

Fig. 2 — Schematic diagram of (a) tensile test standard ASTM E08 specimen, and (b) Test samples at different orientations to rolling direction.

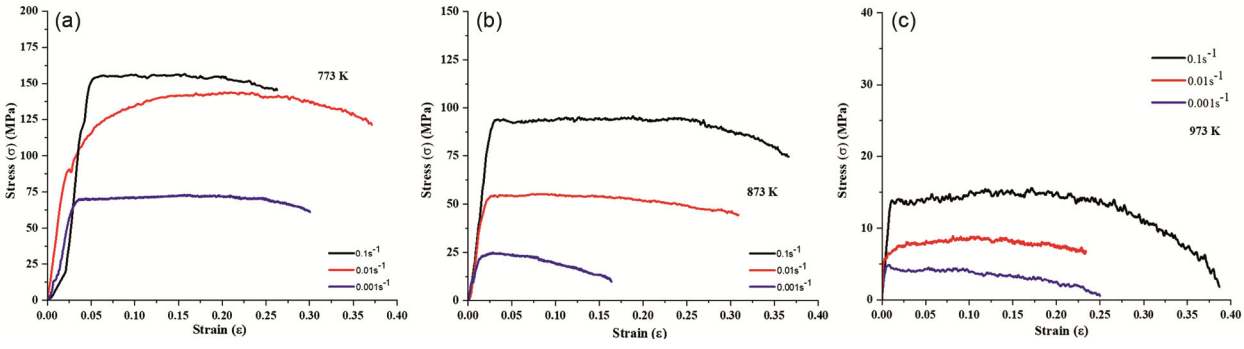

Fig. 3 — Effect of temperature on stress-strain curves at (a) 773K, (b) 873K, and (c) 973K in rolling direction.

Table 1 — Average mechanical properties of Brass alloy

Temperature	Orientation	YS (MPa)	UTS (MPa)	% elongation	In-plane Anisotropy (A_{IP})	Anisotropy index (δ)
773 K	0º	127	126	43	0.06693	0.0487
	45º	120	126	39		
	90º	117	123	36		
873K	0º	93	75	36	0.022567	0.0746
	45º	71	51	32		
	90º	73	53	31		
973K	0º	15	12	39	0.02667	0.06849
	45º	12	10	35		
	90º	10	11	34		

strength decreases with a rise in temperature. This is mainly due to an obvious softening phenomenon, especially at higher test temperature. Decrease in yield stress is mainly because of thermal activation of dislocation motion[19]. Table 1 gives calculated material properties of Brass.

Due to inherent anisotropic nature of sheet, material properties vary with respect to atomic spacing variance within crystallographic orientations. Lankford coefficient generally characterizes this plastic anisotropy of metal. This parameter is generally calculated as per ASTM 517-00:2010 standard[20]. Different anisotropic factors, namely, normal & planer anisotropy, Lankford coefficients, and in-plane anisotropy were usually calculated. It has been mentioned in literature that normal and planar anisotropy parameters are sensitive. There are some other robust stress-based parameters, namely in-plane anisotropy (A_{IP}) and anisotropic index (δ). Jata et al.[21] proposed an in-plane anisotropy (A_{IP}) constraint regarding yield stress variation. It is expressed as

$$A_{IP} = \frac{2\times\sigma_{ys}^{0}-\sigma_{ys}^{90}-\sigma_{ys}^{45}}{2\times\sigma_{ys}^{0}} \quad \ldots (1)$$

A rise in values of A_{IP}, designates a rise in amount of anisotropic nature. The A_{IP} values for Brass were evaluated and listed in Table 1. Further, Wu and Koo[22] suggested anisotropy behavior in terms of total % elongation. It defined as anisotropic index δ. It is represented as Eq.2. A drop in anisotropic index δ isdetected with Brass's rise in test temperature (Table 1).

$$\delta = \frac{(\%El)^{0}-(\%El)^{90}}{(\%El)^{0}+(\%El)^{90}}, 0 \le \delta < 1 \quad \ldots (2)$$

3 Results and Discussion

3.1 Johnson-Cook (JC) model

Johnson-Cook (JC) model requires fewer parameters and a simple expression than other accessible models. Thus, JC model is one of most commonly used constitutive models. This model describes material's dynamic mechanical behavior and quasi-static deformation across a wide range of strain rates[23]. According to JC model, flow stress expression is as follows:

$$\sigma = (A + \mathrm{B}\varepsilon^{\mathrm{n}})\left(1 + \mathrm{C}\ln\frac{\dot{\varepsilon}}{\dot{\varepsilon}_{\mathrm{ref}}}\right)\left(1 - \left(\frac{T-\mathrm{T_{ref}}}{T_m - T_{ref}}\right)^{m}\right) \quad \ldots (3)$$

where, σ stands for flow stress, A stands for yield strength at reference temperature (T_{ref}) and strain rate ($\dot{\varepsilon}_{\mathrm{ref}}$), ε is plastic strain, $\frac{\dot{\varepsilon}}{\dot{\varepsilon}_{ref}}$ is dimension-less plastic strain rate, B is coefficient of strain hardening and $T\&T_m$ are absolute and melting temperature of alloy respectively. The pervious studied experimental results indicated that deformation temperature, strain, and strain rate combined influence material's flow stress behavior[24]. On other hand, original Johnson-Cook model takes temperature, strain, and strain rate into account independently. JC model's accuracy suffers as a result of this assumption[24]. A minor change to original model that links effects of temperature, strain, and strain rate has been proposed to address this issue. Mathematical expression for m-JC model is,

$$\sigma = (\mathrm{A_1} + \mathrm{B_1}\varepsilon + \mathrm{B_2}\varepsilon^{2})\left(1 + \mathrm{C_1}\ln\frac{\dot{\varepsilon}}{\dot{\varepsilon}_{\mathrm{ref}}}\right)\exp\left[(\lambda_1 + \lambda_2\ln\frac{\dot{\varepsilon}}{\dot{\varepsilon}_{\mathrm{ref}}})(\mathrm{T}-\mathrm{T_{ref}})\right] \quad \ldots (4)$$

where A_1, B_1, B_2, C_1, λ_1, λ_2 are material constants. m-JC model captures combined impact of strain rate and temperature and strain and temperature, whereas original JC model does not. Following steps are followed to calculate material constants:

Step I

At reference temperature (25ºC) and strain rate ($0.001s^{-1}$), Eq. 4 is reduced to:

$\sigma = (A_1 + B_1\varepsilon + B_2\varepsilon^2)$

Values of A_1, B_1 and B_2 are evaluated from σ vs ε plot and values are summarized in Table 2.

Step II

At reference temperature (25ºC), Eq. 4 is reduced to:

$$\frac{\sigma}{(A_1 + B_1\varepsilon + B_2\varepsilon^2)} = \left(1 + C_1 \ln \frac{\dot{\varepsilon}}{\dot{\varepsilon}_{ref}}\right)$$

value of C_1 is obtained by $\frac{\sigma}{(A_1+B_1\varepsilon+B_2\varepsilon^2)}$ vs $\ln\frac{\dot{\varepsilon}}{\dot{\varepsilon}_{ref}}$ plot.

Step III

After rearranging terms and considering natural logarithm on both sides of Eq. 4, equation reduce to

$$\ln\left\{\frac{\sigma}{(A_1+B_1\varepsilon+B_2\varepsilon^2)\left(1+C_1\ln\frac{\dot{\varepsilon}}{\dot{\varepsilon}_{ref}}\right)}\right\} = \left(\lambda_1 + \lambda_2 \ln \frac{\dot{\varepsilon}}{\dot{\varepsilon}_{ref}}\right)(T - T_{ref})$$

In complete strain range, linear fitting gives three different values corresponds to specific strain rate. The values of λ_1 and λ_2 are estimated from $\left(\lambda_1 + \lambda_2 \ln \frac{\dot{\varepsilon}}{\dot{\varepsilon}_{ref}}\right)$ vs $\ln\left(\frac{\dot{\varepsilon}}{\dot{\varepsilon}_{ref}}\right)$ plot. Thus, all of material constants of m-JC model were evaluated and listed in Table 2. An equation for m-JC model for Brass is,

$$\sigma = (105.4 + 45.3\varepsilon - 12.7\varepsilon^2)\left(1 + 0.000084 \ln \frac{\dot{\varepsilon}}{0.01}\right) \exp\left[(-0.0001 + 0.0003 \times \ln \frac{\dot{\varepsilon}}{(0.01)})(T - 25)\right.$$

Table 2 — Material constants for m-JC constitutive model

A_1 (MPa)	B_1	B_2	C_1	λ_1	λ_2
105.4	45.3	12.7	0.000084	-0.0001	0.0003

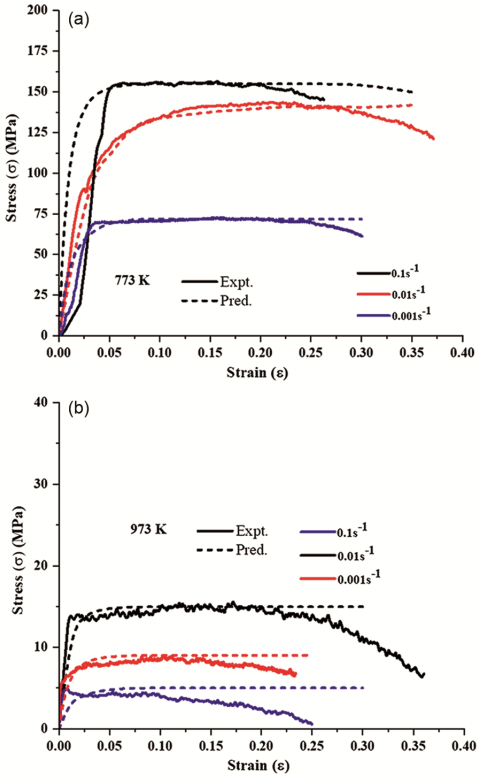

Fig. 4 — Comparison between experimentally measured and predicted flow stress for different strain rates by m-JC model (a) 773K, and (b) 973K.

Capability of m-JC model was estimated by comparing experimental and predicted flow stresses. Figure 4 signifies comparative flow stress behavior at different strain rates and test temperatures m-JC model.

In m-JC model (Fig. 4(a-b)), prediction is better than JC model except at RT condition. Correlation coefficientstatistical metrics is used to compare appropriateness of constitutive models (R = 0.9215). For comparison, other statistical metrics such as average absolute error (Δ) and its standard deviation (s) are used. The m-JC model had lower absolute error value and a lower standard deviation. Above comparison is based on average absolute error (Δ = 7.65 %) and its standard deviation (s = 9.67 %). Because m-JC is a phenomenological model, it does not take into account physical characteristics of materials such as dislocation movement, slip kinetics, and different thermodynamic factors when estimating flow stress.

3.2 Anisotropic Yield Criteria

3.2.1 Hill 1948 Yield Criterion

Hill[25] suggested a planar anisotropy extension of von Mises yield function. By means of plastic hardening modulus and yield stress, material yielding reaction is represented as an elastic-plastic constitutive relationship. An anisotropic yield function is,

$$2\tilde{\sigma}^2 = (G + H)\sigma_{11}^2 + (F + H)\sigma_{22}^2 - 2H\sigma_{11}\sigma_{22} + 2N\sigma_{12}^2 \quad \ldots (5)$$

here, F,G,H and N are anisotropic material coefficients which are expressed as

$$G = \left(\frac{2}{1 + r_0}\right)\left(\frac{\sigma_e}{\sigma_0}\right)^2$$

$$F = \left(\frac{2r_0}{r_{90}(1 + r_0)}\right)\left(\frac{\sigma_e}{\sigma_0}\right)^2$$

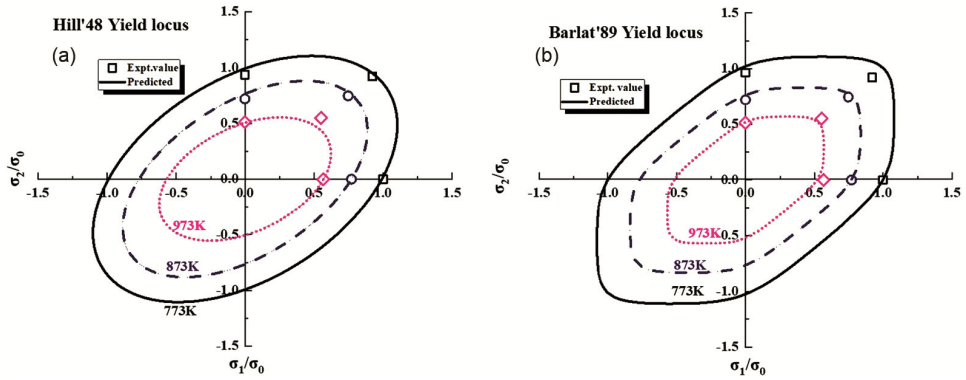

Fig. 5 — Yielding loci of Brass with using (a) Hill 1948, and (b) Barlat 1989 criteria.

$$H = \left(\frac{2r_0}{1+r_0}\right)\left(\frac{\sigma_e}{\sigma_0}\right)^2$$

$$N = \left(\frac{(r_0+r_{90})(r_{30}+r_{60}+1)}{r_{90}(1+r_0)}\right)\left(\frac{\sigma_e}{\sigma_0}\right)^2$$

Here, r_0, r_{45}, r_{90} are anisotropic/ Lankford coefficient, σ_e & σ_0 yield strength values. Anisotropic parameter are calibrated as per steps followed by Mahalle et al. [26] and listed in Table 3.

3.2.2 Barlat 1989 Yield Criterion

Anisotropic yield function equation established by Barlat and Lian [27] in plane stress condition, is stated as

$$2\tilde{\sigma}^m = a|k_1+k_2|^m + a|k_1-k_2|^m + c|2k_2|^m = \phi \quad \ldots (6)$$

here, k_1 and k_2 can be represented by means of yield strength as

$$k_1 = \frac{\sigma_1 - h\sigma_2}{2} \; k_2 = \sqrt{\left(\frac{\sigma_1 - h\sigma_2}{2}\right)^2 - p^2\tau_{12}^2}$$

In Eq. 6, anisotropy ratio functions a, c & h are expressed as

$$a = 2\left(1 - \sqrt{\frac{r_0 r_{90}}{(1+r_0)(1+r_{90})}}\right) \; h = \sqrt{\frac{r_0(1+r_{90})}{r_{90}(1+r_0)}} \; c = (2 - a)$$

Here, r_0&r_{90} anisotropic/ Lankford coefficient, p value is considered iteratively by varying Lankford parameter with respect to angle θ from 0°, is expressed as,

$$r_\theta = \frac{2m\sigma_0^m}{\sigma_\theta\left(\frac{\theta\phi}{\partial\sigma_{11}} + \frac{\partial\phi}{\partial\sigma_{22}}\right)} - 1 \quad \ldots (7)$$

Where, angle θ is considered as 45º to relate p-value. An anisotropic parameter are calibrated as per a systematic method followed by Mahalle et al.[26] and listed in Table 4.

Table 3 — Calibrated material parameters in Hill1948 yielding function

Temperature (K)	N	F	H	G
773K	3.5981	2.1401	0.8246	1.1754
873 K	3.4728	1.9045	0.8595	1.1405
973K	3.1254	2.3145	0.8024	1.1902

Table 4 — Calibrated material parameters in Barlat'89 yielding function

Temperature (K)	a	c	H	P
773K	0.9389	1.0611	1.1756	1.4
873 K	0.7679	1.2321	1.1252	1.4
973K	1.0618	0.9382	1.2175	1.4

Figure 5 gives yield loci plotted by Hill 1948 and Barlat 1989 yield criteria for all test temperatures. It is noticed that Barlat 1989 yield function shows closeness to experimental data point as Hill 1948 yield function is unable to capture yield behavior of Brass. Thus, Barlat 1989 yield function shows a better prediction of yield behavior of Brass at all test temperatures.

4 Conclusion

Following are major conclusions drawn from present study:

- Hot tensile flow stress behaviors have been affected significantly by test temperatures and strain rates for Brass alloy.
- Drop-in yield and ultimate tensile strength have been observed at approximately 58 % and 68 % with a rise in test temperature from 773 K to 973 K. Around 30% improvement has been observed in % elongation with rise in test temperature.
- Predictions capability of uniaxial constitutive equations, namely m-JC equations, have been evaluated using coefficient of correlation, average absolute error, and root mean square error.

- Further, yield loci have been plotted at various temperatures using Hill 1948 and Barlat 1989 yield function. Barlat 1989 has followed experimental results correctly in all test temperature.

References

1 Wright RN, *Wire Technol Process Eng Metall,* (2016).
2 Ratnayaka DD, Brandt MJ, & Johnson KM, *Water Supply,* (2009).
3 Green DE, Neale KW, MacEwen SR, Makinde A, & Perrin R, *Int J Plast,* 20(2004) 1677.
4 Gupta K, Jain NK, & Laubscher R, *Adv Gear Manuf Finishing Classical Mod Processes,* (2017).
5 Rehren T, *J Archoelogical Sci,* 26(1999) 1083.
6 Singh VD, Mahalle G, Kotkunde N, Singh SK, & Hussain MM, *Adv Mater Process Technol,* (2021) 1.
7 El-Danaf E, Kalidindi SR, Doherty RD, & Necker C, *Acta Mater,*48(2000) 2665.
8 Kalidindi SR, *Int J Plast,* 17*(*2001) 837.
9 Fan R, Magargee J, Hu P,& Cao J, *Mater Sci Eng A,* 574(2013) 218.
10 Duggan BJ, Hatherly M, Hutchinson WB, & Wakefield PT, *Met Sci,* 12(1978) 343.
11 Asgari S, El-Danaf E, Kalidindi SR& Doherty R.D, *Metall Mater Trans A Phys Metall Mater Sci,* 28(1997) 1781.
12 Sakharova NA, Fernandes JV & Vieira MF, *Mater Sci Eng A*507(2009) 13.
13 Mahalle G, Kotkunde N, Shah R, Gupta AK, & Singh SK, *J Phys Conf Ser,* 1063 (2018) 1.
14 Mahalle G, Kotkunde N, Kumar Gupta A, & Kumar Singh S, *Mater Today Proc,* 5 (2018) 18016.
15 Mohammed AAS, El-Danaf EA, & Radwan AKA, *Mater Sci Eng A,* 457 (2007) 373.
16 Xiao YH, Guo C, & Guo XY, *Mater Sci Eng, A*528 (2011) 6510.
17 Padmavardhani D, & Prasad YVRK, *Metall Trans A,* 22 (1991) 2993.
18 Fang XT, He GZ, Zheng C, Ma XL, Kaoumi D, Li YS, & Zhu YT, *Acta Mater,* 186 (2020) 644.
19 Dieter G.E, *Mech Metall SI Metr Edition,* (2011).
20 ASTM 517-00:2010 Stand Test Method for Plastic Strain Ratio r for Sheet Metal. *ASTM B. Stand,* (2010) 1.
21 Jata K V, Hopkins AK, & Rioja RJ, *Mater Sci Forum,* 217 (1996) 647.
22 Wu YT, & Koo CH, *Scr Mater*, 38 (1997) 267.
23 Johnson G, & Cook W, *Eng Fract Mech,* 21 (1985) 31.
24 Mahalle G, Kotkunde N, Gupta AK, Sujith R, Singh SK, & Lin YC, *J Mater Eng Perform,* 28 *(*2019) 3321.
25 Hill R, *J Mech Phys Solids,* 38 (1990) 405.
26 Mahalle G, Salunke O, Kotkunde N, Gupta AK, & Singh SK, In ASME Int Mech Eng Congress Exposition, (2019) 1.
27 Barlat F, & Lian K, *Int J Plast,* 5 (1989) 51.